Layered Structure of Langmuir–Blodgett Polymer Films Measured by Interlayer Energy Transfer

Satoru Ohmori, Shinzaburo Ito, and Masahide Yamamoto*

Department of Polymer Chemistry, Faculty of Engineering, Kyoto University, Sakyo-ku, Kyoto 606, Japan

Received June 26, 1990; Revised Manuscript Received November 5, 1990

ABSTRACT: The layered structure of Langmuir–Blodgett (LB) films of poly(vinyl octal) (PVO) has been investigated by the time-resolved fluorometry of the energy transfer between layers containing energy donor and acceptor moieties. The poly(vinyl octal)s containing phenanthrene and anthracene chromophores (P and A polymers) were synthesized by the acetalization of poly(vinyl alcohol) with octanal and chromophoric aldehyde. The polymer was spread onto pure water and transferred by dipping a quartz plate vertically. The samples ($P(n)A$), which consisted of two layers of P polymer, n layers of PVO, and two layers of A polymer (n = 0–8) were prepared for fluorescence measurements. The transfer ratio was unity for all the films, and the thickness measured by ellipsometry was proportional to the number of layers. Although the surface film was deposited on the substrate well, energy-transfer efficiency for each P(n)A was larger than the theoretical value predicted by Förster mechanism. This indicates the structural relaxation of the layered polymer films. Assuming Gaussian distribution of the chromophores, the theoretical decay functions for the phenanthrene fluorescence were calculated by the Monte Carlo method according to the Förster mechanism and then were fitted with the observed decay curves. The procedure enabled quantitative evaluation of the partly disordered structure of the polymer LB films. Fluorescence analysis based on the interlayer energy transfer is quite sensitive to microscopic change of the film structure in the molecular dimension.

Introduction

Recently, extensive investigations on Langmuir–Blodgett (LB) films have been made on the design and the construction of functional thin films.[1] In the field of photophysics and photochemistry, Kuhn and his co-workers have studied fundamental photophysical processes, such as energy transfer and electron transfer in LB films,[2] and they have used these processes as tools to reveal the structural properties of the LB film. They constructed an interlayer energy-transfer system with the long-chain fatty acids using the cyanine dye molecule as the hydrophilic moiety. They reported that the Förster theory[3] can be successfully applied to describe the energy-transfer phenomena observed by photostational measurements.[4] However, some recent studies show that the experimental results of interlayer energy transfer are often out of keeping with the Förster theory. Particularly, Fromherz and Reinbold extended Kuhn's experiments using various fatty acids with different chain lengths in order to change the distance of separation between chromophoric layers.[5] They concluded that the Förster theory is not adequate for real systems, and that time-dependent measurements must be made to determine the reason for the misfit.

Energy transfer to acceptor molecules reduces the emission probability of donor molecules, resulting in reduced fluorescence intensity and in a shortened decay time. If a system contains molecules under various situations, e.g., different location and orientation in a polymer matrix, the system exhibits a multiexponential fluorescence decay as the sum of different dissipation rates. Thus, analyses of the fluorescence decay curves give further information on the spatial distribution of chromophores. However, in the study of LB films, this has been difficult due to the short lifetimes of cyanine dyes and the weak intensity of the extremely thin films. Fortunately both the sensitivity and the time resolution have been improved by the recent development of optical instruments, e.g., laser and photon counting systems. These instruments enable us to analyze specimens of LB films consisting of only a few layers.

Leitner et al. first analyzed the energy transfer in a LB system by picosecond time-resolving measurements with a streak camera.[6] In their study, the fluorescence decay of the interlayer energy-transfer system was not fitted with the theoretical prediction for the two-dimensional energy-transfer system. Then they suggested that the transient decay analysis of the energy-transfer process gives information on the geometrical molecular arrangements in an LB film.

Yamazaki et al. conducted studies on energy transfer by time-resolved fluorescence spectroscopy using the picosecond single-photon-counting technique.[7] Although the system showed stepwise energy transfer from a donor to acceptors, the chromophores in LB films of fatty acids aggregated in the two-dimensional plane and showed a fractal distribution. They concluded that the control of the fractal distribution is one of the key points in constructing photofunctional LB films.

Recently, some preformed polymers were found to form a stable monolayer at the air–water interface and to be transferable to solid substrate.[8–25] One of these polymers is the poly(vinyl octal) reported by Ogata et al.[25] Using this as a base polymer, we succeeded in realizing uniform chromophore distribution in a two-dimensional plane, in which the chromophores are linked to the polymer chain with covalent bonds.[26]

The main purpose of this study is a quantitative analysis of the interlayer energy-transfer process as a probing technique of the layered structure of polymer LB films. To this end, phenanthrene and anthracene moieties were introduced into this polymer as an energy donor and an energy acceptor chromophore, respectively. The energy transfer was observed by the single-photon-counting system, and the observed decay curve was fitted with the theoretical function, which was calculated by the Monte Carlo method with the assumption that in the direction of film thickness the chromophores take a distribution around the original position deposited. These fluorescence analyses made clear the structural relaxation of polymer LB films.

0024-9297/91/2224-2377$02.50/0

Scheme I

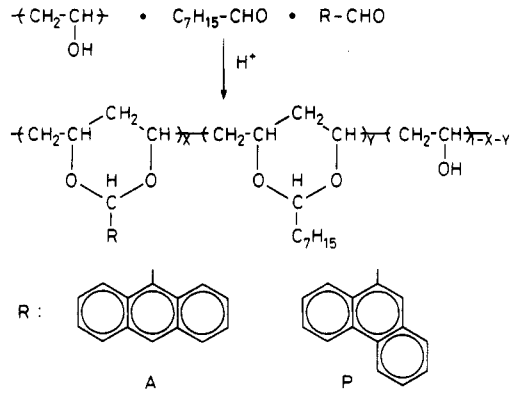

Experimental Section

Sample Preparation. Poly(vinyl octal)s with chromophoric groups were synthesized by the acetalization of commercial poly(vinyl alcohol), as shown in Scheme I, according to the procedure of Ogata et al.[25] Poly(vinyl alcohol) (PVA; DP = 2000) 0.5 g; Wako Pure Chemical Industries, Ltd.) and a mixture of octanal (Wako) and a chromophoric aldehyde (anthracenecarbaldehyde or phenanthrenecarbaldehyde purchased from Aldrich Chemical Co., Inc.) were dissolved in 10 mL of chloroform, and two drops of hydrochloric acid was added as the catalyst. The reaction mixture was stirred for 15–24 h at 40 °C. The PVA powder dissolved as the acetalization proceeded. The solution was poured into 500 mL of methanol containing a chip of sodium hydroxide. The polymer was purified by reprecipitation from benzene into methanol three times and freeze-dried from benzene solution. The residue of unreacted chromophores (small-molecule contaminant) in the polymer sample was monitored with UV absorbance of anthracenecarbaldehyde (the extinction coefficient at 403 nm was determined to be 6750 L mol^{-1} cm^{-1}) at each step of reprecipitation. After the alkaline methanol treatment, the dried polymer contains 6×10^{-2} mol L^{-1} anthracenecarbaldehyde in the bulk. But the first reprecipitation decreases the concentration to 4×10^{-4} mol L^{-1}. After the succeeding purifications, we could not detect the absorption of the anthracenecarbaldehyde. From these results, it can be safely said that the amount of residual contaminant is less than 10^{-5} mol L^{-1} in the polymer bulk, which is low enough for the following fluorescence measurements of the labeled polymers.

Table I shows the synthesized polymers and the amount of reactant aldehydes. Three kinds of polymer were prepared; nonchromophoric polymer (PVO) for the spacing layer, phenanthrene polymer (P1) for the energy-donating layer, and anthracene polymer (A1, A2) for the energy-accepting layer. The compositions of chromophoric unit and octal unit were represented by X and Y, respectively (see Scheme I).

The extinction coefficient of anthracene units was determined as follows, and it was used to calculate the fraction of anthracene units in the polymer. Here the isomers of 4,6-dimethyl-2-(9-anthryl)-1,3-dioxane (DMAD), a model compound of the anthracene unit, were synthesized from the isomeric mixture of 2,4-pentanediol and anthracenecarbaldehyde. 2,4-Pentanediol (1.0 g) and anthracenecarbaldehyde (5 g; Aldrich) were dissolved in 20 mL of chloroform. In the presence of three drops of hydrochloric acid, the solution was stirred at 40 °C overnight. After the addition of alkaline (NaOH) methanol, the mixture was extracted with dichloromethane. The products were purified twice by column chromatography on silica gel with dichloromethane as eluent and by recrystallization from hexane. The obtained compounds were a mixture of meso and racemic DMAD: mp 169 °C; ^1H NMR (CD_2Cl_2) δ 1.35 (d, methyl), 1.6–1.9 (m, methylene), 4.0–4.4 (m, methine), 6.9 (s, methine), 7.3–8.9 (m, aromatic). Anal. Calcd for $C_{20}H_{20}O_2$: C, 82.16; H, 6.90; O, 10.94. Found: C, 82.15; H, 6.88; O, 10.92. The extinction coefficient of the anthracene unit was determined to be 8880 L mol^{-1} cm^{-1} at 364 nm by dissolving DMAD in dichloromethane. The extinction coefficient of the phenanthrene group was also determined to be 11 750 L mol^{-1} cm^{-1} at 296 nm in dichloromethane by using 9-phenanthrenemethanol. The fractions of octal units and chromophore units in the obtained polymers were calculated from the UV absorbance of chromophores and the carbon fraction in elementary analysis, as listed in Table I.

Water in the subphase was ion-exchanged, distilled, and passed through a water purification system (Barnstead Nanopure II). The benzene solution of acetalized polymer (0.01 wt %) was dropped on the surface of pure water (18–19 °C) in a Teflon-coated trough (Kenkosha SI-1). The surface film was compressed at the rate of 1 cm min^{-1}. The surface pressure–area isotherm was recorded by using a Wilhelmy-type film balance (Shimadzu ST-1). A nonfluorescent quartz plate (1 cm × 4 cm) was used as a solid substrate for the fluorescence measurements. The quartz plate was cleaned in sulfuric acid containing a small amount of potassium permanganate, dipped in 10% hydrogen peroxide solution, then washed with pure water thoroughly, and made hydrophobic by submersion in a 10% solution of trimethylchlorosilane in toluene for 20 min. Silicon wafers, used for ellipsometry, were cleaned by chloroform. The surface film was transferred to the substrate at a surface pressure of 25 mN m^{-2} for PVO, 22.5 mN m^{-2} for P1, and 21.0 mN m^{-2} for A1 by dipping the substrate vertically at the rate of 1.5 cm min^{-1}. For the silicon wafer, the film was transferred only in an up mode, but at the following dips the deposition took place both in up and down modes to form a Y-type built-up film with the transfer ratio of unity. For the hydrophobic quartz plate, the deposition was possible in both modes from the first layer.

Figure 1 illustrates the structure of LB films for energy-transfer measurements. On a quartz plate, 18 layers were deposited in the following order: (1) 4 layers of the PVO in order to prevent the effect of the interface of the substrate, (2) 2 layers of P1 as the energy-donating layers, (3) 0–8 layers of PVO as the spacer of chromophores, (4) 2 layers of A1 as the energy-accepting layers, and (5) PVO layers whose number was adjusted so that the total number of layers became 18. These samples have the same number of layers and the same composition of P1, A1, and PVO polymers. Besides these, PVO layers from 1 to 41 layers were deposited on silicon substrates in order to measure the thickness by ellipsometry, and P1 layers from 2 to 30 layers were deposited on quartz plates to determine the linear relationships of fluorescence intensity and absorbance against the number of layers. Before fluorescence measurements, the samples were allowed to stand for 1 week in a desiccator in order to remove the structural instability at an early stage after the deposition.

Measurements. UV-absorption spectra were measured by a Shimadzu UV-200S spectrophotometer. Fluorescence spectra and excitation spectra were recorded by a Hitachi 850 fluorescence spectrophotometer. The spectral response was calibrated with a standard tungsten lamp. A single-photon-counting method was used for the measurement of fluorescence decay curves and time-resolved fluorescence specta.[27,28] The pulsed excitation light was obtained with a Spectra-Physics picosecond synchronously pumped, mode-locked, cavity-dumped dye laser (Models 2020, 342A, 375B, 344S). The emission through a diffuser and monochromator was detected with a photomultiplier (Hamamatsu R3234). The time-correlated pulses were obtained by conventional Ortec photon-counting electronics and accumulated on a multichannel analyzer (Norland IT-5300) controlled with a microcomputer (NEC 9801). The full-width at half-maximum of the overall excitation pulse was 500 ps. The obtained fluorescence decay was analyzed by the least-squares method with a computer (NEC 9801). To eliminate the polarization effect, magic angle excitation was adopted for the decay curve measurements according to Spencer and Weber.[29] The theoretical fluorescence decay curves were simulated by the Monte Carlo method with a computer (Fujitsu M382). The film thickness was measured by a Mizojiri Kogaku ellipsometer.

Results and Discussion

Surface Pressure–Area Isotherms. Figure 2 shows the surface pressure–area (F–A) isotherms of the acetalized polymers on pure water. As the surface film is compressed, the surface pressure increased sharply at the area of ca. 1 m^2 mg^{-1} and the monolayer collapsed by further compression in the plateau region. The limiting areas per

Table I
Amount of Reactant Aldehydes, Composition of Polymers, and Areas of Acetal Units

sample	octanal, g	phenanthrene-carbaldehyde, g	anthracene-carbaldehyde, g	carbon fractn, %	X,[a] %	Y,[b] %	Z, %	$X/(X+Y)$, %	area of acetal,[c] nm²/unit	area of acetal,[d] nm²/unit	area of acetal,[e] nm²/unit
PVO	4.00	0	0	71.31	0	73	27	0	0.35	0.27	0.33
P1	1.50	2.40	0	73.14	12	57	31	17	0.34	0.27	0.33
A1	1.79	0	1.65	71.92	7.1	55	38	12	0.32	0.29	0.35
A2	0.45	0	4.60	74.20	17	58	25	23			

[a] Compositions of chromophoric acetal unit (see Scheme I). [b] Compositions of octal unit (see Scheme I). [c] Limiting area of acetal units, assuming that the area of the alcohol unit is 0.12 nm². [d] Area at the transferred surface pressure, assuming that the area of tha alcohol unit is 0.12 nm². [e] Area at the transferred surface pressure, assuming that the area of the alcohol unit is negligible.

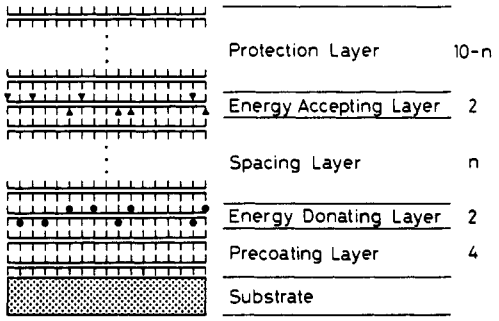

Figure 1. Schematic illustration of the multilayer structure of the LB films used for photophysical measurements. Circles represent the phenanthrene chromophores; triangles represent the anthracene chromophores.

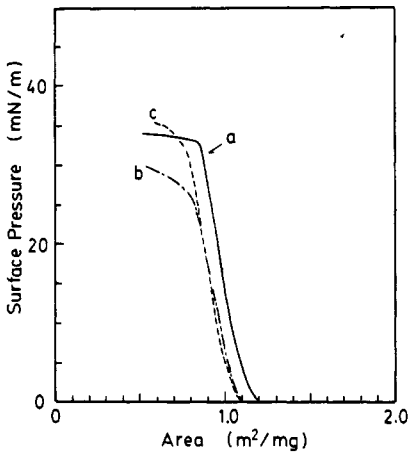

Figure 2. Surface pressure–area isotherms of poly(vinyl octal)s containing chromophores at 19 °C. (a) PVO, (b) P1, and (c) A1.

unit weight of A1 and P1 slightly decreased compared with that of PVO, because the molecular weight of chromophoric units is larger than the octyl units. Here the limiting area was defined as that in which the steepest line of the F–A isotherm is extrapolated to zero surface pressure. The F–A isotherm of A2 was not reproducible and the obtained line shows a very small limiting area. Probably, the surface film of A2 is not a monolayer due to aggregation of the anthracene units. Under the assumption that the limiting area of the vinyl alcohol unit is 0.12 nm²,[25] the limiting area of acetal units was calculated and listed in Table I. The limiting areas of acetal units in PVO and P1 are in the range of 0.34–0.36 nm², as was reported by Ogata et al.[25] The surface film of A1 shows a slightly small limiting area for the acetal unit. In this case, the alcohol units slip into water as a result of the higher alcohol fraction (Z = 38% in Table I).[25] The areas of acetal units at the transferred surface pressure are also shown in Table I, assuming that the area of the alcohol unit is 0.12 nm². These values are too small for the rigid acetal units. Then, with the assumption that the area of

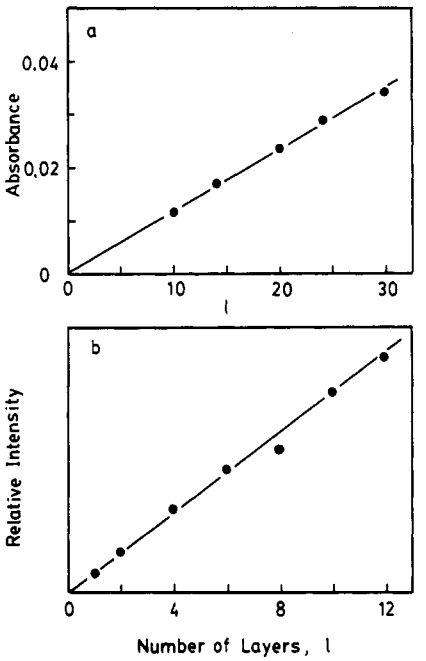

Figure 3. UV absorbance of built-up films as a function of number of layers (on one side). (a) UV absorbance of P1 at 298 nm and (b) fluorescence intensity of P1 at 350 nm.

the alcohol unit is equal to zero, the areas of acetal units at the transferred pressure became close to the limiting area of acetal units, as shown in Table I. These values are in reasonable agreement with the value of 0.32 nm² derived from the molecular model: the main chain lies in the plane parallel to the water surface and the side chains are oriented upside to the plane normal.[25] Since the alcohol units are flexible and more hydrophilic than the acetal units, this assumption that the area of the alcohol unit is negligible at the transferred pressure seems plausible. The values in the last column were used for evaluating the plane density of chromophoric units and the lattice size of a plane in a chromophore distribution.

Deposition of Surface Film onto Solid Substrates. To verify the deposition of surface film to the substrate, the absorbance of transferred LB film was measured. Figure 3a shows the relation between the absorbance of P1 films at 298 nm and the number of layers. Although the range of absorbance values is limited and the values are very small, the absorbance appears to be proportional to the number of layers. To check the linear relationship for the LB films having small numbers of layers, fluorescence intensity was measured (Figure 3b). The fluorescence intensity also increased proportionally with the number of layers. That is, stable deposition of the surface films occurred, at least up to 30 layers.

Next, the thickness of the transferred films was measured by ellipsometry for various numbers of layers of deposition. The errors inherent in this measurement are

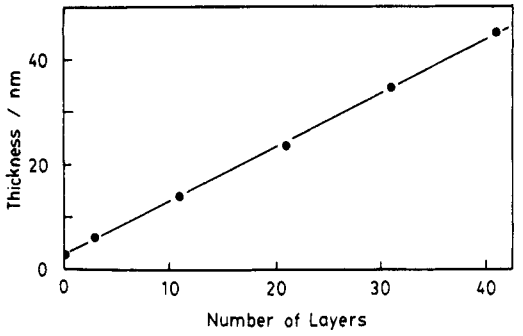

Figure 4. Film thickness of PVO as a function of number of layers. The thickness at the 0 layer shows the value of the oxidized silicon layer located at the wafer surface.

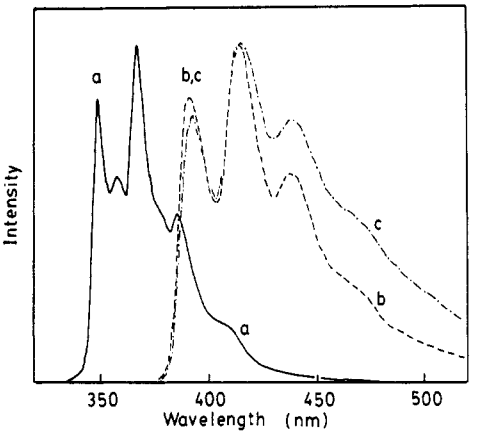

Figure 5. Fluorescence spectra of two-layer LB films. (a) P1, (b) A1, and (c) A2. Spectra are recorded with the excitation wavelength of 298 nm and the bandwidth of 3 nm.

of the order of a few percent. Figure 4 shows the relation between the number of layers and the thickness of the LB film. The thickness at 0 layer shows the value of the oxidized silicon layer located at the surface of the wafer. There is a linear relationship between the number of layers and the film thickness. The thickness of one layer, d_{sp}, is calculated to be 1.02 nm from the slope of the line. This value is much smaller than that of conventional fatty acids. The monolayer is stabilized by both the hydrophilic main chain and hydrophobic side chain, which is not required to be a long alkyl chain. The thinness is one of the most important characteristics of polymer LB film. This means that the incorporated chromophores can easily carry out energy transfer between neighboring layers.

These macroscopic measurements, fluorescence intensity, absorbance, and ellipsometry, show that the surface film can be stably transferred onto the substrates.

Fluorescence Spectra. Figure 5 shows the fluorescence spectra of two-layer LB films. The emission of A1 at 393, 416, and 438 nm is the monomer fluorescence of the anthracene chromophore; these values are almost the same as that of the model compound in dilute solution. In the case of A2, structureless broad emission is superimposed on the monomer emission. This broad emission is probably due to excimer formation between anthracene chromophores.[30] The F–A isotherm of A2 gave too small a limiting area, as described before. Thus, the anthracene groups seem to aggregate in the surface film of the A2 polymer. Hence, A1 was used for the energy-accepting layer, although the concentration of anthracene units is not enough to achieve perfect quenching of excited phenanthrene in neighboring layers. The emission of P1 at 350, 357, 367, and 387 nm is the monomer fluorescence of the phenanthrene group, and the spectrum indicates that there

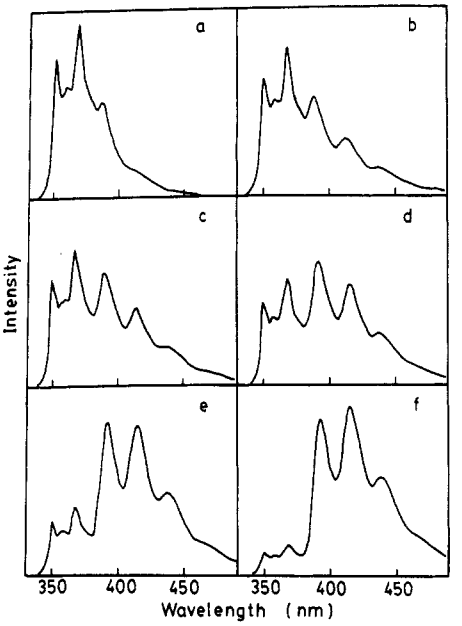

Figure 6. Fluorescence spectra of P(n)A films. (a) P, (b) P8A, (c) P6A, (d) P4A, (e) P2A, and (f) P0A. Spectra are recorded with the excitation wavelength of 298 nm and the bandwidth of 3 nm.

is no specific interaction between phenanthrene groups both in the ground state and in the excited state.

Interlayer Energy Transfer. The radius of energy transfer (Förster radius) is usually a few nanometers for various pairs of energy donors and acceptors,[31] and the thickness of polymer LB films is in the range of these radii. Therefore, the energy-transfer system is well constructed by the layered structure of these polymer LB films. Conversely, microscopic analyses of the layered structure of polymer LB films are possible by observing the energy transfer between the layers.

PVO layers were sandwiched as spacers between two chromophoric layers and the energy transfer between the phenanthrene and anthracene layers was measured. Hereafter, these films are called P(n)A films. P and A mean the two layers of phenanthrene polymer (P1) and the two layers of anthracene polymer (A1), respectively, and n is the number of spacer layers. For example, P2A indicates the sample of $n = 2$ in Figure 1.

Figure 6 shows the fluorescence spectra of these films. Of course, P shows only phenanthrene emission. As the number of spacer layers is reduced from 8 to 0, the intensity of phenanthrene emission decreases, and in place of it, anthracene emission increases at the longer wavelengths. This means that the excitation energy of the phenanthrene unit transfers to the anthracene unit over the spacer layers and that the efficiency is controlled by the layer thickness.

Figure 7 shows the relative intensity, I/I_0, vs the number of spacing layers, where I is the intensity of phenanthrene emission of P(n)A at 350 nm and I_0 is that of P at 350 nm. At this wavelength there is no spectral overlap with the anthracene emission. Therefore we can easily evaluate the quenching efficiency from the ratios of I/I_0. For a sample of P(n)A, the mean distance between two chromophoric layers is expressed by $(n+2)d_{sp}$, as seen in Figure 1. Therefore the abscissa of Figure 7 is $n + 2$. The Förster radius between phenanthrene group and anthracene group was calculated from the fluorescence spectrum of D and the absorption spectrum of A as follows:

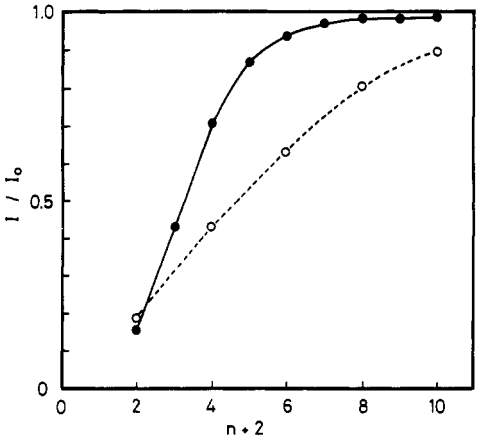

Figure 7. Intensities of phenanthrene emission of P(n)A films (at 350 nm) relative to the unquenched sample, P, as a function of the number of spacing layers. Open circles represent the observed values and closed circles represent the theoretical values calculated by Förster mechanism.

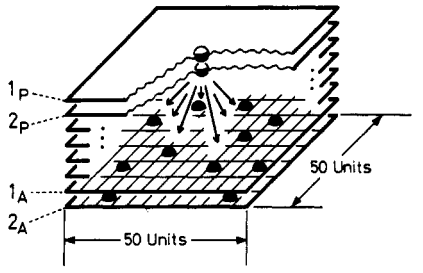

Figure 8. Schematic illustration of the model for the calculation by Monte Carlo method. White balls and black balls represent phenanthrene and anthracene chromophores, respectively. Arrows mean energy transfer from the phenanthrene to the anthracene unit.

$$R_{DA} = [(9000 \ln 10\, K^2 \Phi_D) J/(128\pi^5 n^4 N)]^{1/6} \quad (1)$$

$$J = \int F_D(\lambda)\epsilon_A(\lambda)\lambda^4\, d\lambda \quad (2)$$

where K is the orientation factor, n is the refractive index of the medium, Φ_D is the quantum efficiency of donor D, $F_D(\lambda)$ is the fluorescence spectrum normalized such that $\int F_D(\lambda)\, d\lambda = 1$, and $\epsilon_A(\lambda)$ is the extinction coefficient of A at wavelength λ. The calculated values of R_{DA} for P and A units is 2.12 nm. Considering the Förster radius of the present pair, the relative intensity I/I_0 should be much larger (almost unity for P8A; the mean distance is 10.2 nm) that the experimentally obtained values, 0.9. To understand this result, the values of I/I_0 were simulated in the following way.

At first, to obtain the theoretical values of I/I_0 for given arrangements, the decay function of phenanthrene emission was calculated; the details of the calculation are shown in the next section. Then, the values of I/I_0 were calculated from the integral of obtained decay function and shown in Figure 7 by the solid line. The observed ratio of the P0A is close to the theoretical one. However, for the sample of $n + 2 = 4$, the measured value is much smaller than the theoretical value, and the difference is still large for the other samples.

Structural Model for Theoretical Treatment and Simulation of Fluorescence Decay. To elucidate the precise behavior of the interlayer energy transfer, the fluorescence decay curves were measured by the single-photon-counting technique with a picosecond laser pulse. The theoretical decay curves were also obtained by the Monte Carlo method. The model of the system is shown in Figure 8.

(1) The phenanthrene chromophore is set in the center of a plane. The donor phenanthrene chromophores exist in two adjacent layers. Then the energy-transfer rates from the first layer to the anthracene layers (from 1_P to 1_A and 2_A), and from second layer (from 2_P to 1_A and 2_A), were calculated alternatively.

(2) In the direction of film thickness, the chromophores were assumed to be located in the middle of each chromophoric layer. Then the distances D between layers of donors and acceptors were calculated by the following equation.

$$D = (n + k)d_{sp} \quad (3)$$

Here, d_{sp} is the thickness of one layer, which is equal to 1.02 nm, n is the number of spacers from 0 to 8, and k = 1 for $2_P \rightarrow 1_A$, $k = 2$ for $1_P \rightarrow 1_A$ and $2_P \rightarrow 2_A$, and $k = 3$ for $1_P \rightarrow 2_A$.

(3) The anthracene units are randomly distributed in a lattice of acetal units. The unit size of lattice was assumed to be the size of the acetal units at the transferred pressure, as described previously. The calculated lattice is 50 × 50 units: this size is large enough since the results were not affected even when a 100 × 100 unit area was used.

(4) All distances between a phenanthrene and the randomly distributed anthracene chromophores were calculated. Then the energy-transfer rates corresponding to the distances were calculated by the Förster formula. These calculations were repeated for 1000 patterns of random distribution of anthracene units. The obtained 1000 decays were added and the sum was normalized.

Calculation of the energy-transfer rates was based on the following assumptions.

(1) Energy transfer occurs by dipole–dipole interaction expressed by the Förster formula[3]

$$W_{DA} = (R_{DA}/r_{DA})^6/\tau_D \quad (4)$$

where W_{DA} is the probability of energy transfer per unit time from an excited donor molecule D to an acceptor molecule A, r_{DA} is the distance between D and A, and R_{DA} is the critical transfer radius (Förster radius 2.12 nm), at which donor D has an equal probability of energy transfer to other decay processes, and τ_D is the unquenched lifetime of D (43 ns).

(2) The dipole moments of chromophores are randomly oriented.

(3) Energy migration between phenanthrene groups can be neglected.

The validity of the Förster formula is widely accepted.[7] We separately synthesized a poly(vinyl octal) containing both the phenanthrene and anthracene chromophores and checked the energy-transfer mechanism by using the thick film cast on a quartz plate. The fluorescence decay curve of phenanthrene precisely agreed with the Förster formula derived for a three-dimensional system. This result also justifies that the energy migration between phenanthrene chromophores can be neglected under the experimental condition that the average distance between phenanthrene units (1.38 nm) is much larger than the Förster radius (0.87 nm).[30] In previous work, we demonstrated that a statistically random distribution of chromophores can be achieved in a plane of LB film prepared from PVO, where the chromophores are randomly attached to the polymer chain with covalent bonds.[26] This point is another characteristic of the polymer LB film besides the thinness of each layer.

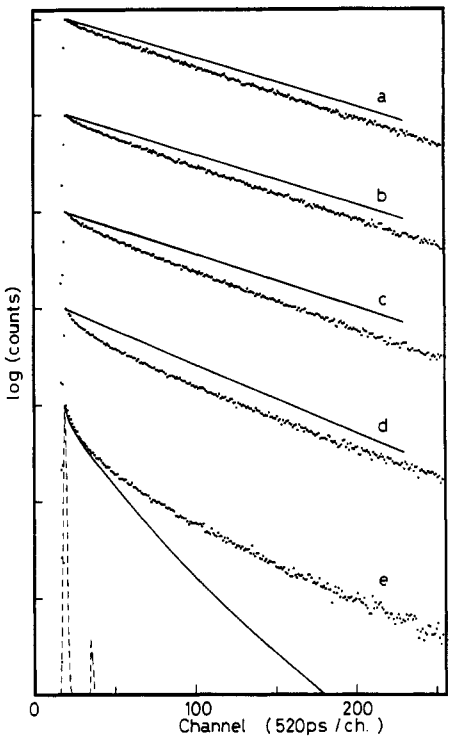

Figure 9. Observed decay curves of the phenanthrene emission of P(n)A films and the convoluted theoretical lines calculated by Monte Carlo method. (a) P8A, (b) P6A, (c) P4A, (d) P2A, and (e) P0A. The emission is monitored at wavelength of 357 nm with the excitation wavelength of 298 nm. The broken line shows the instrument response function.

Figure 9 shows that the observed fluorescence decays did not fit with the calculated ones. P0A shows a slower decay curve, but others show faster decay components in the early time range. This deviation is partly due to the small amount of contamination of the emission from PVO layers, which have no chromophores but show weak fluorescence with a short lifetime of ca. 1.6 ns in the observed wavelengths with the excitation at 298 nm. The decay curve of P should be a single-exponential function, but the actual curve can be fitted with a sum of exponentials; the main component with a lifetime of 43 ns is easily assigned to the phenanthrene emission, but the minor one with a lifetime of ca. 1.6 ns is assigned to the emission from PVO layers. To obtain a good fit with the observed data of P, 1% of this extraneous emission needs to be included. On the decay analyses for P(n)A samples, this minor emission cannot be ignored, because the number of layers of PVO is ~10 times that of the P layers, and the lifetime is rather short. We tried to analyze the observed decays including the component from PVO layers. However, the fitness was not improved except for that of sample P. In this study, to derive the theoretical function, a random orientation of chromophores is assumed. A preferential orientation may cause the deviation of the decay curves. To prove this point, the orientation of chromophore was measured in LB films of PVO by means of the fluorescence polarization technique. As a fluorescence probe, a fluorene group was introduced to PVO in the same way. Fluorene is a good probe for the polarization measurements, because this group has a high fluorescence anisotropy in solid matrices. The obtained data strongly suggested a random orientation of dipole moments both in the in-plane and the out-of-plane directions. So it seems that the deviation is not caused by molecular orientation.

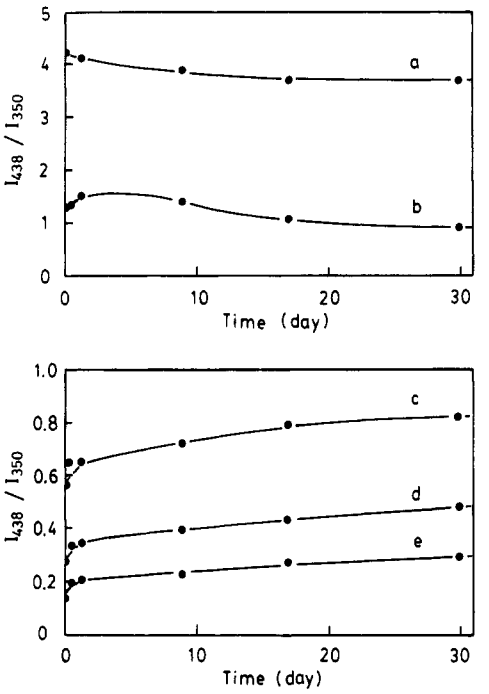

Figure 10. Aging effect on the ratio of fluorescence intensities at 350 (phenanthrene emission) and 438 nm (anthracene emission) for P(n)A films. (a) P0A, (b) P2A, (c) P4A, (d) P6A, and (e) P8A.

Another possibility is structural relaxation of the layered films. Figure 10 shows the aging effect on the ratio of fluorescence intensities at 350 (phenanthrene emission) and 438 nm (anthracene emission). P4A, P6A, and P8A show rapid increase of energy-transfer efficiency at the early stage after deposition. After 1 day, the speed of increase drops. On the other hand, P0A shows a continuous decrease of energy-transfer efficiency. This phenomenon is related to the structural relaxation of polymer LB films. The results are explained as follows. For the films of P4A, P6A, and P8A, the distances between phenanthrene and anthracene units decrease and the efficiency of energy transfer increases. For the P0A film, the distance continues to increase because the chromophores are initially arranged to the nearest position. In the case of P2A, both effects appear.

As a result of the structural relaxation due to the segmental diffusion of the polymer chain, the chromophores do not stay in the original plane deposited. In this case, the fluorescence decay curve deviates from the theoretical calculation based on an ideal two-dimensional distribution of chromophores. All the measurements were carried out 1 week after the deposition, since the newly made samples were not stable for a few days.

Evaluation of the Disordered Layer Structure. To estimate the degree of disordering, the fluorescence decay curve of phenanthrene was analyzed by a theoretical model including chromophore distribution in the direction of plane normal. As a model of chromophore distribution, a Gaussian function, $G(d)$, was employed:

$$G(d) = [(2\pi)^{1/2}s)]^{-1} \exp[-(d - m)^2/2s^2] \quad (5)$$

Here d is the position of chromophore in the direction normal to a layer plane, m is the average value of d, and s is the standard deviation. Figure 11 shows the chromophore distributions at various s. At $s = 0$ the chromophores are distributed only at the deposited plane. With the increase of s, the distribution becomes wider and the peaks merge into one peak. The Monte Carlo calculation was again made under these distributions. Then the

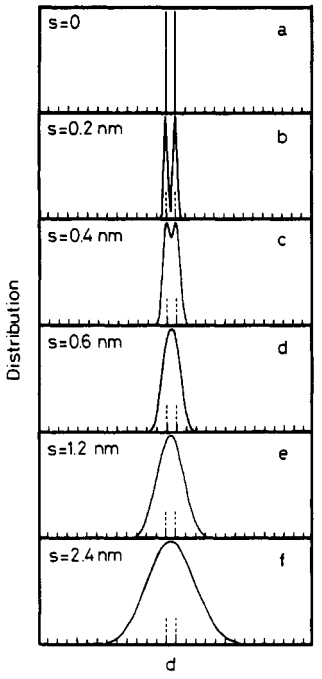

Figure 11. Chromophore distribution with Gaussian functions for various standard deviations. Broken lines in abscissa represent the position of layers under the assumption that the layer structure is not disordered.

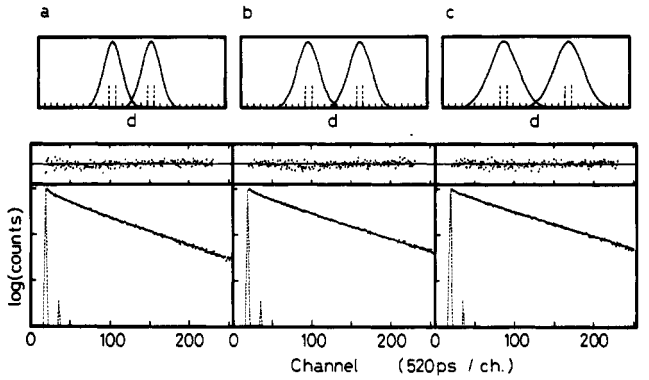

Figure 12. Decay curve fitting for P(n)A films by the Monte Carlo method, assuming the Gaussian distrubition of chromophores, and the obtained distribution of chromophores. (a) P4A (s = 1.35 nm), (b) P6A (s = 1.70 nm), and (c) P8A (s = 2.25 nm). The residual plots are shown in the upper part of the decay curves. The full scale is ±10.

fluorescence decay curves were fitted with the calculated functions by use of the least-squares method. This operation was repeated for various values of s to obtain the best values of s for fitting.

Curve fitting was successful for the samples with 4, 6, and 8 spacer layers. The best fit values of s were obtained to be 1.35, 1.70, and 2.25 nm for P4A, P6A, and P8A, respectively. The minimum values of the mean square of the residuals (χ^2) were 1.72, 1.64, and 1.67, respectively. Although these values seem to be somehow large compared to the multiexponential decay analysis, the curve fitting was successful with such a simple model. Figure 12 shows the result of curve fitting by this model and the distribution of chromophores in the LB films for the obtained values of s. This result shows that the layer structure is fairly disordered in polymer LB films. Although macroscopic measurements such as UV absorption and ellipsometry show no change before and after aging, the fluorescence analysis based on the interlayer energy transfer is quite sensitive to microscopic change of the film structure in the molecular dimension.

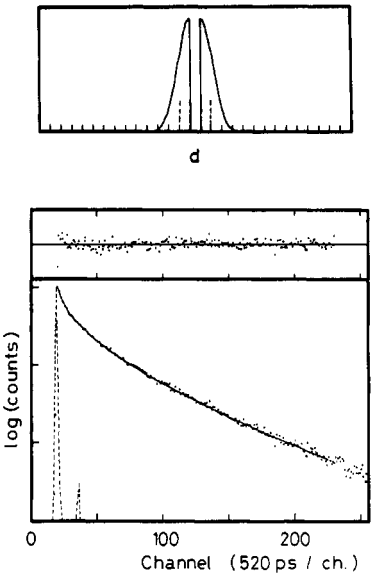

Figure 13. Decay curve fitting for P0A films by the Monte Carlo method, assuming the refined Gaussian distribution under a reflecting boundary condition, and the obtained distribution of chromophores. s = 0.83 nm. The full scale of residual plots is ±10.

If the original structure was in layered planes and then relaxed as the result of molecular motion, the values of s should not depend on the number of spacer layers. However, the obtained values of s increase with the spacer number. There are two possibilities for the cause of this increase, as follows.

(1) Some structural defects, such as pinhole or bilayer of polymer chain, originally exist in the surface film on water or at the deposition. In this case, the distribution of the distance becomes larger with the number of layers piled up.

(2) The structural relaxation in the spacing layers is larger than that in the chromophoric layers. Then the distance distribution between the chromophoric layers become large with the increasing of spacer layers.

In this study, the latter is mainly responsible for the increase of s value, since aging was observed after the deposition. It is easily supposed that the aromatic chromophores are more rigid than the alkyl side chains. In fact, the glass transition temperatures of poly(vinyl octal)s become high as the fraction of chromophoric unit increases.[26c]

For the films of P0A, decay curve fitting with the Gaussian distribution of chromophores was a failure. P0A film shows a slower decay than the ideal model (see Figure 9e), and analysis with the Gaussian function gives a progressively faster decay with increase of the s value. In the Gaussian model, the anthracene unit can penetrate into the phenanthrene layer. However, it seems natural that the anthracene and phenanthrene units cannot approach each other within their molecular sizes, since each group is directly attached to the different polymer chains with rigid acetal bonds. Therefore, we analyzed P0A by the refined model in which the spatial mixing of chromophores was inhibited. The nearest distance between anthracene and phenanthrene units is set to the thickness of one layer, 1.02 nm, and the Gaussian distribution under a reflecting condition at the boundary of P and A was adopted. Then the simulation was done with various values of s to fit with the fluorescence decay curve. Figure 13 shows the decay curve fitting by these best fit parameters and the distri-

bution of chromophores for the fitted value of s. The decay curve is successfully fitted with this distribution model.

Conclusion

LB films containing the phenanthrene and anthracene chromophores were prepared from a preformed polymer, poly(vinyl octal). The thickness of the monolayer is quite thin, i.e., ca. 1 nm, which is in the radius of energy transfer between various chromophores. The energy-transfer phenomenon between the layers gives us information on the structure of polymer LB films. The fluorescence decay curves of phenanthrene are measured by the single-photon-counting technique and simulated by the Monte Carlo method, assuming the relaxation of layered structure. This procedure enabled quantitative evaluation of the degree of disordering of the layered structure. The results are summarized as follows.

(1) The thickness of deposited film linearly increases with the number of layers. For the polymers containing chromophoric units, the fluorescence intensity and UV absorbance are also proportional to the number of layers. From these macroscopic measurements, the surface film on water is quantitatively transferred to the substrate.

(2) Although the deposition was carried out smoothly, the disordered structure was detected by measuring the energy-transfer behavior of donor fluorescence. This means that the energy transfer is one of the most sensitive ways to investigate the layer structure of LB films.

(3) Structural relaxation of the layered films was manifested in situ through the energy-transfer phenomenon. In addition to some initial distortion of layer structure, appreciable increase of transfer efficiency occurs during a few days after the deposition. This aging effect shows that segmental diffusion takes place in the LB films.

Acknowledgment. We thank Drs. Y. Yonezawa and M. Kawasaki (Department of Industrial Chemistry, Faculty of Engineering, Kyoto University) for their kind measurements of ellipsometry. This work was partially supported by a Grant-in-Aid for Scientific Research (No. 01550692) and a Grant-in-Aid for Scientific Research on Priority Areas, New Functionality Materials-Design, Preparation and Control (No. 01604567), from the Ministry of Education, Science and Culture of Japan.

References and Notes

(1) (a) *Thin Solid Films* **1989**, *178–180*. (b) *Thin Solid Films* **1988**, *159–160*.
(2) (a) Kuhn, H.; Möbius, D.; Bücher, H. In *Physical Methods of Chemistry*; Weissberger, A.; Rossiter, B. W., Eds.; Wiley: New York, 1972; Vol. 1, Part 3B, p 577. (b) Möbius, D. *Ber. Bunsenges. Phys. Chem.* **1978**, *82*, 848. (c) Kuhn, H. *J. Photochem.* **1979**, *10*, 111. (d) Kuhn, H. *Pure Appl. Chem.* **1981**, *53*, 2105.
(3) Förster, Th. *Z. Naturforsch.* **1949**, *4A*, 321.
(4) Kuhn, H. *J. Chem. Phys.* **1970**, *53*, 101.
(5) Fromherz, P.; Reinbold, G. *Thin Solid Films* **1988**, *160*, 347.
(6) Leitner, A.; Lippitsch, M. E.; Draxler, S.; Riegler, M.; Aussenegg, F. R. *Thin Solid Films* **1985**, *132*, 55.
(7) (a) Yamazaki, T.; Tamai, N.; Yamazaki, I. *Chem. Phys. Lett.* **1986**, *124*, 326. (b) Yamazaki, I.; Tamai, N.; Yamazaki, T. *J. Phys. Chem.* **1987**, *91*, 3572. (c) Tamai, N.; Yamazaki, T.; Yamazaki, I. *J. Phys. Chem.* **1987**, *91*, 841. (d) Tamai, N.; Yamazaki, T.; Yamazaki, I. *Chem. Phys. Lett.* **1988**, *147*, 25. (e) Yamazaki, I.; Tamai, N.; Yamazaki, T.; Murakami, A.; Mimuro, M.; Fujita, Y. *J. Phys. Chem.* **1988**, *92*, 5035.
(8) Breton, M. *J. Macromol. Sci., Rev. Macromol. Chem.* **1981**, *C21(1)*, 61.
(9) (a) Takenaka, T.; Harada, K.; Matsumoto, M. *J. Colloid Interface Sci.* **1980**, *73*, 569. (b) Takeda, F.; Matsumoto, M.; Takenaka, T.; Fujiyoshi, Y. *J. Colloid Interface Sci.* **1981**, *84*, 220.
(10) (a) Tredgold, R. H.; Winter, C. S. *J. Phys. D: Appl. Phys.* **1982**, *15*, L55. (b) Tredgold, R. H.; Winter, C. S. *Thin Solid Films* **1983**, *99*, 81. (c) Vickers, A. J.; Tredgold, R. H.; Hodge, P.; Khoshdel, E.; Girling, I. *Thin Solid Films* **1985**, *134*, 43. (d) Winter, C. S.; Tredgold, R. H.; Vickers, A. J.; Khoshdel, E.; Hodge, P. *Thin Solid Films* **1985**, *134*, 49. (e) Tredgold, R. H. *Thin Solid Films* **1987**, *152*, 223.
(11) Naito, K. *J. Colloid Interface Sci.* **1989**, *131*, 218.
(12) (a) Kakimoto, M.; Suzuki, M.; Konishi, T.; Imai, Y.; Iwamoto, M.; Hino, T. *Chem. Lett.* **1986**, 823. (b) Nishikata, Y.; Kakimoto, M.; Imai, Y. *J. Chem. Soc., Chem. Commun.* **1988**, 1040.
(13) (a) Kawaguchi, T.; Nakahara, H.; Fukuda, K. *J. Colloid Interface Sci.* **1985**, *104*, 290. (b) Kawaguchi, T.; Nakahara, H.; Fukuda, K. *Thin Solid Films* **1985**, *133*, 29.
(14) (a) Matsumoto, M.; Itoh, T.; Miyamoto, T. In *Cellulosics Utilization*; Inagaki, H., Phillips, G. O., Eds.; Elsevier: London, 1989; p 151.
(15) Mumby, S. J.; Swalen, J. D.; Rabolt, J. F. *Macromolecules* **1986**, *19*, 1054.
(16) (a) Laschewsky, A.; Ringsdolf, H.; Schmidt, G.; Schneider, J. *J. Am. Chem. Soc.* **1987**, *109*, 788. (b) Ringsdolf, H.; Schmidt, G.; Schneider, J. *Thin Solid Films* **1987**, *152*, 207. (c) Schneider, J.; Ringsdolf, H.; Rabolt, J. F. *Macromolecules* **1989**, *22*, 205. (d) Schneider, J.; Erdelen, C.; Ringsdolf, H.; Rabolt, J. F. *Macromolecules* **1989**, *22*, 3475.
(17) Carpenter, M. M.; Prasad, P. N.; Griffin, A. C. *Thin Solid Films* **1988**, *161*, 315.
(18) (a) Murakata, T.; Miyashita, T.; Matsuda, M. *Macromolecules* **1988**, *21*, 2730. (b) Murakata, T.; Miyashita, T.; Matsuda, M. *Macromolecules* **1989**, *22*, 2706.
(19) (a) Seki, T.; Ichimura, K. *Polym. Commun.* **1989**, *30*, 108. (b) Seki, T.; Tamaki, T.; Suzuki, Y.; Kawanishi, Y.; Ichimura, K.; Aoki, K. *Macromolecules* **1989**, *22*, 3505. (c) Seki, T.; Ichimura, K. *Thin Solid Films* **1989**, *179*, 77.
(20) Era, M.; Kamiyama, K.; Yoshiura, K.; Momii, T.; Murata, H.; Tokito, S.; Tsutsui, T.; Saito, S. *Thin Solid Films* **1989**, *179*, 1.
(21) Tamura, M.; Ishida, H.; Sekiya, A. *Thin Solid Films* **1989**, *178*, 373.
(22) Kumehara, H.; Kasuga, T.; Watanabe, T.; Miyata, S. *Thin Solid Films* **1989**, *178*, 175.
(23) Nerger, D.; Ohst, H.; Schopper, H.-C.; Wehrmann, R. *Thin Solid Films* **1989**, *178*, 253.
(24) Lupo, D.; Prass, W.; Scheunemann, U. *Thin Solid Films* **1989**, *178*, 403.
(25) (a) Oguchi, K.; Yoden, T.; Sanui, K.; Ogata, N. *Polym. J.* **1986**, *18*, 887. (b) Watanabe, M.; Kosaka, Y.; Sanui, K.; Ogata, N.; Oguchi, K.; Yoden, T *Macromolecules* **1987**, *20*, 452. (c) Watanabe, M.; Kosaka, Y.; Oguchi, K.; Sanui, K.; Ogata, N. *Macromolecules* **1988**, *21*, 2997. (d) Oguchi, K.; Yoden, T.; Kosaka, Y.; Watanabe, M.; Sanui, K.; Ogata, N. *Thin Solid Films* **1988**, *161*, 305.
(26) (a) Ito, S.; Okubo, H.; Ohmori, S.; Yamamoto, M. *Thin Solid Films* **1989**, *179*, 445. (b) Ohmori, S.; Ito, S.; Yamamoto, M.; Yonezawa, Y.; Hada, H. *J. Chem. Soc., Chem. Commun.* **1989**, 1293. (c) Ohmori, S.; Ito, S.; Yamamoto, M. *Macromolecules* **1990**, *23*, 4047.
(27) O'Connor, D. P.; Phillips, D. *Time-Correlated Single Photon Counting*; Academic: London, 1984.
(28) Yamazaki, I.; Tamai, N.; Kume, H.; Tsuchiya, H.; Oba, K. *Rev. Sci. Instrum.* **1985**, *56*, 1187.
(29) Spencer, R. D.; Weber, G *J. Chem. Phys.* **1970**, *52*, 1654.
(30) (a) Hargreaves, J. S.; Webber, S. E. *Macromolecules* **1984**, *17*, 235. (b) Itoh, M.; Fuke, K.; Kobayashi, S. *J. Chem. Phys.* **1980**, *72*, 1417. (c) De Schryver, F. C.; Boens, N.; Huybrechts, J.; Daemen, J.; De Brackeleire, M. *Pure Appl. Chem.* **1977**, *49*, 237.
(31) Berlman I. B. *Energy Transfer Parameters of Aromatic Compounds*; Academic: New York, 1973.